Review Article

Renyin Zhang, Xuejing Wang, Xiaoyu Ma, Zhihua Xu, Mingze Ma, Tieying Zhang, and Feng Shi*

Advances in the synthesis of gold nanoclusters (AuNCs) of proteins extracted from nature

https://doi.org/10.1515/ntrev-2023-0193
received April 22, 2023; accepted December 31, 2023

Abstract: Over the past few decades, nanotechnology has developed rapidly and has been applied to various fields. Gold nanoclusters (AuNCs), which are composed of several hundred atoms, are a new type of nanomaterial. AuNCs are often synthesized using ligands or templates. The interaction between the gold atoms and the groups of the ligands or templates results in unexpected physical and chemical properties. In recent studies, natural proteins have often been used as templates to synthesize AuNCs. The unique structure of natural proteins endows AuNCs with biological functions, such as biocompatibility and enzymatic activity. The unique properties of these natural protein-AuNCs have been verified and applied in various fields. In this article, the synthetic strategies used to produce AuNCs have been divided into two categories: animal-derived and plant-derived protein synthesis. The protein types and synthesis strategies used in the current mainstream research are reviewed, and their applications in detection and biological imaging are summarized. Finally, the problems and future development directions of AuNCs synthesized from natural proteins are discussed, laying a foundation for the biological application of protein-AuNCs.

Keywords: gold nanocluster, AuNCs, natural protein, synthesis

1 Introduction

Since the invention of the scanning tunneling microscope in 1981, nanotechnology has garnered significant interest. It is used to study the properties and applications of materials with structural dimensions in the range of 1–100 nm [1]. Nanotechnology enables the refinement of properties of matter at atomic and molecular levels. In recent years, various nanostructures such as nanoparticles, nanorods, nanotubes, and nanoclusters have been developed and have potential applications in a wide range of fields [2]. Noble metal nanomaterials have been of particular interest, and metals such as gold [3], silver [4], copper [5], and platinum [6], have been widely explored. Nanoclusters are considered an important subclass of the burgeoning field of nanotechnology, especially as they exhibit properties that differ from those of single nanoparticles. Gold nanoclusters (AuNCs) are clustered nanostructures with core sizes of less than 10 nm and are composed of several hundreds of metal atoms [7]. AuNCs are often synthesized in the presence of ligands. The interactions between these ligand groups and metal atoms lead to increased stability of the clusters and unique properties [8]. However, there are still some shortcomings in the preparation of AuNCs, such as the need to improve their stability to prevent aggregation [9]. Different ligands, such as thiol compounds and dendritic molecules, are used as stabilizers to synthesize AuNCs [10]. However, some ligands, such as 4-tert-butylthiophenol and 1-thioglycerol, require more complex synthesis processes or are harmful to the environment [11]. Moreover, some AuNCs exhibit low stability, pH sensitivity, and low water solubility [12]. These shortcomings have hindered the development of AuNCs. Recently, biosynthetic methods have gradually emerged to overcome the shortcomings of AuNCs. Different types and sources of proteins have been used to synthesize AuNCs, such as plants [13,14], plant extracts [15], animal proteins [16], and enzymes [17], and the approach is considered a promising alternative to traditional methods (Figure 1).

Early methods for the synthesis of AuNCs predominantly used chemical reduction methods, which involved several harsh conditions, such as the requirement of organic solvents, strong reducing agents, or high reaction temperatures and times. The process of using natural proteins to synthesize AuNCs often involves mild reaction conditions and does not require the addition of stabilizers or reducing agents. The synthesized protein-AuNCs often emit fluorescence and are non-toxic. This article summarizes the current mainstream methods for the synthesis of AuNCs from

* **Corresponding author: Feng Shi**, College of Life Science, Shihezi University, Shihezi 832003, China, e-mail: shifeng2314@yeah.net, tel: +86-153 0993 8011
Renyin Zhang, **Xuejing Wang**, **Xiaoyu Ma**, **Zhihua Xu**, **Mingze Ma**, **Tieying Zhang:** College of Life Science, Shihezi University, Shihezi 832003, China

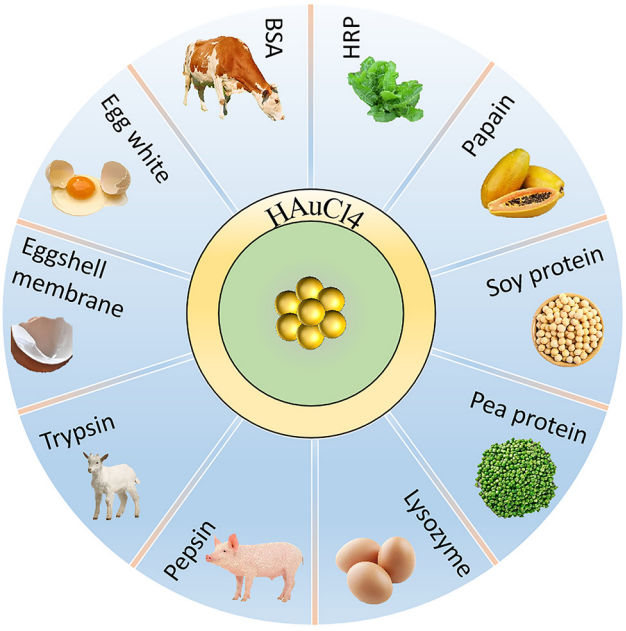

Figure 1: Different natural sources of protein.

natural proteins, as well as their latest applications in various fields, such as bioimaging, catalysis, and temperature sensing. This lays a foundation for future research on the protein synthesis of AuNCs and their potential applications.

2 Synthesis of AuNCs from natural proteins

Protein-AuNCs synthesized from natural proteins usually exhibit the physical and chemical properties of AuNCs and the unique physiological properties of proteins, thus combining the unique optical and electronic properties of metal clusters with the biological functions of proteins [18]. The history of AuNCs synthesis using proteins as templates spans nearly 10 years, and because proteins are environmentally friendly and biocompatible, protein-AuNCs can be synthesized using mild reaction conditions. Furthermore, protein-AuNCs have excellent water solubility and stability [19,20]. Here, research has been divided into protein-AuNCs made using proteins from animal and plant sources. Among these, bovine serum albumin (BSA) is the presentative animal-derived protein. The synthesized AuNCs exhibit red emission fluorescence. Owing to their biocompatibility and fluorescence-related characteristics, protein-AuNCs have potential applications in biosensing, bioimaging, and metal ion detection [21,22]. Their good stability, long-term preservation, and resistance to changes in temperature and pH have been demonstrated in numerous studies and are advantages specific to protein-AuNCs. However, the relationship between the protein structure and fluorescence has not yet been elucidated. The fluorescent properties of nanoclusters are affected by the chemical environment in which the nanoclusters exist, their cluster size, and the ligand type used. Presently, it is believed that the generation of fluorescence is mainly due to the quantum size effect triggered by the reduction of gold atom clusters to nanometer sizes. This implies that a perfect template for AuNCs using synthetic proteins or peptides with specified sequences cannot be obtained. In addition to further studying the fluorescence mechanism of protein-AuNCs, the synthesis of more protein-AuNCs will provide useful information regarding their fluorescence, and it is anticipated that such work will provide protein-AuNCs with excellent performance [23].

2.1 Animal-derived proteins

2.1.1 BSA

In many parts of the world, cattle are primarily used as a reliable source of human meat and milk, and their main source of nutrition is protein [24]. The accessibility of bovine proteins and their unique physicochemical properties have prompted researchers to explore their function in AuNC synthesis. BSA is the most abundant plasma protein in serum. Its unique physical and chemical properties are widely used in biology and medicine [25]. BSA is a large globular protein composed of numerous acidic and basic amino acids. These include 35 cysteine residues, which have been proven to reduce and combine to form AuNCs under alkaline conditions [26]. BSA was the first protein used to synthesize protein-AuNCs in 2009 [27]. Its spatial structure provides numerous binding sites for gold, and the 35 cysteine residues maintain strong binding to AuNCs *via* Au-S coordination bonds [28]. Thermogravimetric analysis and matrix-assisted laser desorption ionization mass spectrometry (MALDI-TOF) have shown that the prepared BSA-AuNC core contains 25 gold atoms, which has a typical cluster characteristic and high stability. In addition, the prepared BSA-AuNCs exhibit near-infrared emission characteristics and are very stable under a broad pH range. They can be redispersed in solution and emit strong fluorescence in solid form at room temperature for two months. The pH, temperature, and nature of the reducing agent often have an important influence on the synthesis of protein-AuNCs. Ultraviolet and visible spectrum, X-ray photoelectron spectroscopy (XPS), Fourier transform infrared

spectroscopy (FTIR), and fluorescence spectra have indicated that AuNCs with fewer than eight atoms grow at pH 7–8, whereas clusters with 25 atoms often grow at pH 11 [29]. BSA-stabilized AuNCs provide a good foundation for the synthesis of protein-AuNCs and have promoted their research and exploration. In previous studies, BSA-stabilized AuNCs have been used to detect mercury ions [30]. The detection is based on the specific quenching of BSA-AuNCs fluorescence by mercury ions. Owing to the high quantum yield (QY) and high fluorescence of BSA-AuNCs, the detection limit for mercury ions is only 0.5 nM, which is considerably lower than the recommended minimum mercury content of 10 nM reported by the U.S. Environmental Protection Agency. However, the selectivity and sensitivity of BSA-stabilised AuNCs depend largely on the pH and ionic strength of the sample solution. To solve this, a novel solution was proposed wherein sodium borohydride and ethylene diamine tetraacetic acid were used to inhibit the binding of metal ions to BSA-AuNCs, thereby slowing down the quenching effect and improving selectivity [31]. Other studies have found that Cu^{2+} can inhibit the fluorescence of BSA-AuNCs by interacting with BSA. Furthermore, dopamine can prevent Cu^{2+} from interfering with BSA-AuNCs fluorescence because of its strong Cu^{2+} binding properties. This function has been used for the rapid detection of dopamine [32]. Because of the crucial role of dopamine in neurotransmission, this method could be developed as a sensitive and rapid diagnostic tool. Gold is a typically inert metal in chemistry, and few anions can react with gold. Interestingly, cyanide can form stable gold-cyanide complexes that have strong covalent bonds, resulting in the fluorescence quenching of BSA-AuNCs when cyanide is present [33]. Therefore, BSA-stabilized AuNCs can be subsequently used to detect cyanide. Meanwhile, cystatin C is a protease inhibitor in the human body, widely present in nucleated cells and body fluids. Because of the correlation between its concentration in serum and some diseases, it is considered a new marker of glomerular filtration rate, which can reflect the health of the kidney. A multifunctional fluorescent sensor based on BSA-AuNCs has been demonstrated for the rapid and sensitive detection of cystatin C and papain [34]. The cysteine protease activity of papain catalyzes the fluorescence quenching of BSA-AuNCs; therefore, the method can be applied to detect papain. However, after the addition of cystatin C, the fluorescence of BSA-AuNCs can be restored; therefore, the method can sensitively determine the concentration of cystatin C in the range of 0.025–2.0 μg/mL with the detection limit of 4.0 ng/mL. Catalase is known to be present in almost all living organisms to break down hydrogen peroxide and provide antioxidant defenses enzymatically. Hydrogen peroxide is the substrate of the reaction. Considering the excellent fluorescence quenching performance of hydrogen peroxide on BSA-AuNCs, a series of quantitative detection methods for enzyme substrates such as glucose and uric acid have been developed [35]. Compared to non-enzymatic detection systems, these methods have the advantages of high sensitivity and specificity, showing considerable diagnostic potential. Quantitative determination methods for hydrogen peroxide based on the principle of fluorescence quenching have emerged extensively. However, the mechanism of hydrogen peroxide-induced AuNC fluorescence quenching remains unclear. Previous studies have suggested that the Au–S bond can be broken by hydrogen peroxide, resulting in the fluorescence quenching of AuNCs [36]. However, other studies have shown that the fluorescence quenching of metal nanoclusters is due to the transfer of protein ligands to the core charge of the metal nanoparticles being hindered [37] (Figure 2).

2.1.2 Ovalbumin

In addition to beef and milk, eggs are a main source of protein because they contain essential amino acids for human survival. Eggs are composed of three main components: the egg white, egg yolk, and eggshell. Most of the proteins in eggs are concentrated in egg whites, and there are four main proteins in egg whites that account for approximately 13% of the total mass of egg whites. These include ovalbumin (54%), ovotransferrin (12%), ovoglobulin (11%), and lysozymes (3.4%) [38]. The availability of egg proteins is an advantage for the synthesis of fluorescent nanoclusters. In 2014, egg whites were used as the starting material for preparing fluorescent protein-AuNCs [39]. By mixing egg white with a chloroauric acid aqueous solution at physiological temperature, adjusting the pH to alkaline, and reacting for 12 h, highly fluorescence and water-soluble protein-AuNCs can be obtained. The obtained protein-AuNCs exhibit red photoluminescence [40]. Subsequent studies have optimized the step in a simple and energy-saving manner by changing the reaction conditions to room temperature without stirring. The prepared red-emitting AuNCs have been used as fluorescent sensors for the sensitive detection of hydrogen peroxide [41]. Ovalbumin, the most abundant protein in egg whites, can be used to generate fluorescent protein-AuNCs through efficient synthesis under alkaline conditions. The AuNCs prepared by this method were shown to selectively capture ricin B in very complex samples, including cell lysates, protein mixtures, and powder samples [42]. Each ovalbumin contains six cysteine and ten tyrosine residues, which can

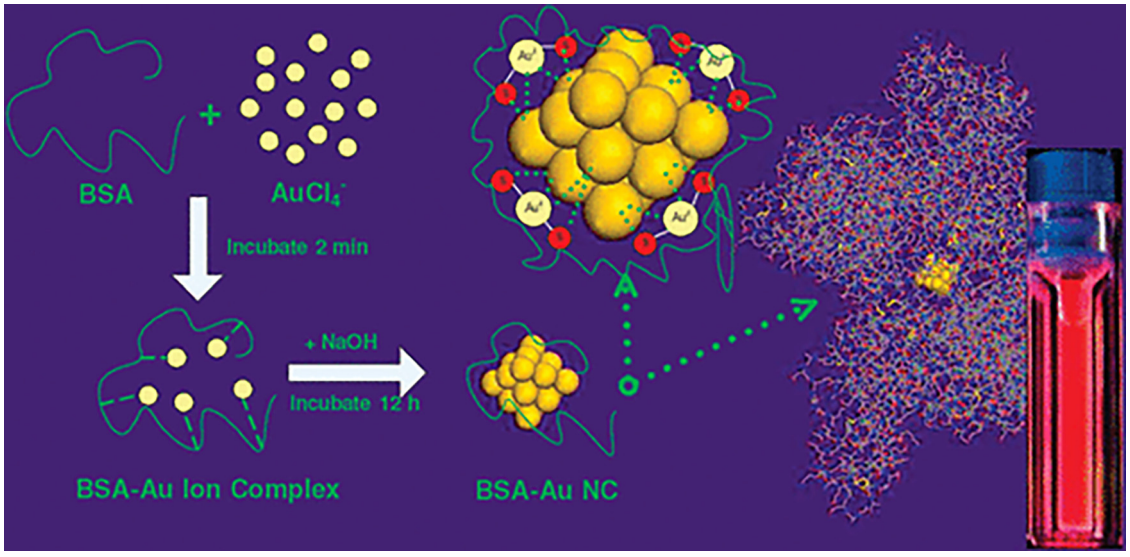

Figure 2: Schematic diagram of AuNCs synthesized by BSA.

reduce and stabilize free gold ions under alkaline conditions [26]. At present, ovalbumin-modified AuNCs can be synthesized using simple and controllable methods. The prepared fluorescent protein-AuNCs exhibit a strong fluorescence emission peak at 650 nm. The prepared clusters have been used as broad-spectrum detectors for real-time detection of tetracycline antibiotics. With an increase in antibiotic concentration, the fluorescence color changes, and the fluorescence intensity at 650 nm decreases [43] (Figure 3).

2.1.3 Eggshell membrane

Most synthetic preparation methods for AuNCs use aqueous solutions. However, biologically derived proteins often exist in solid form. Therefore, researchers investigated whether solid-state proteins could be used as matrix materials for the synthesis of fluorescent protein-AuNCs. The eggshell membrane is an example of a solid form of protein. It is a double-layered insoluble water film with a natural fiber network

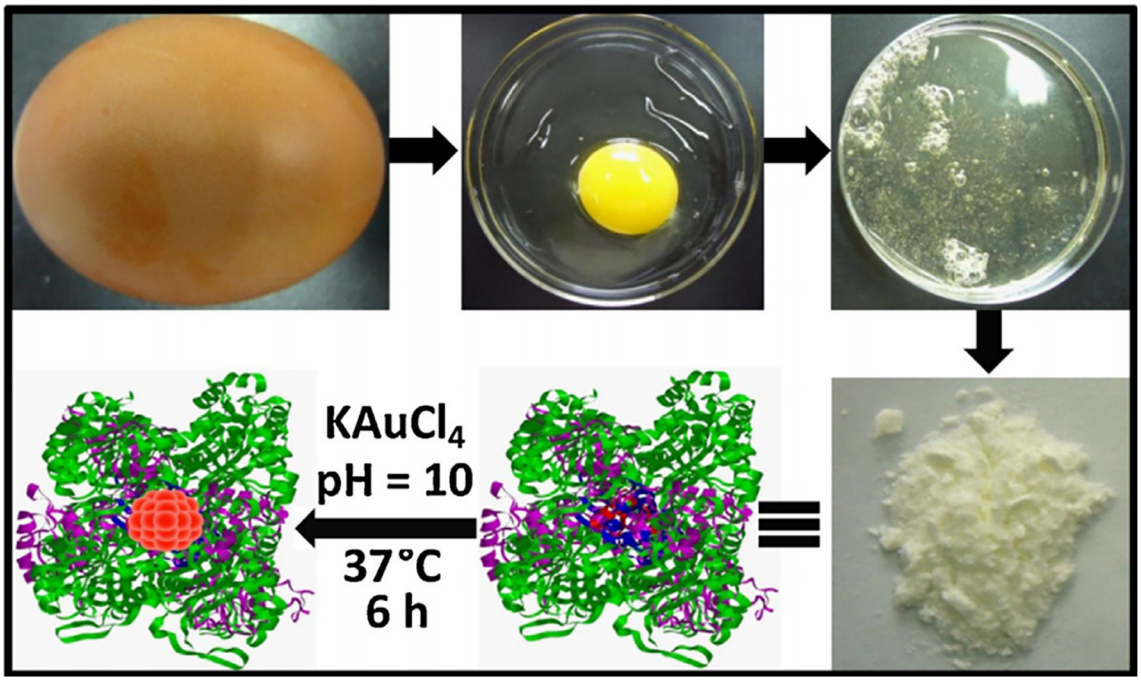

Figure 3: Schematic diagram of AuNCs synthesized by egg albumin.

naturally generated in the eggshell and is composed of highly crosslinked cysteine-rich proteins with a structure similar to that of keratin, collagen, or elastin. As a good supplement to existing methods, a synthetic method for preparing red fluorescent AuNCs was successfully developed using an eggshell membrane as a reducing agent and stabilizer [44]. Meanwhile, AuNCs with peroxidase-like properties have been prepared using eggshell membranes as templates. First, ESM-AuNCs were combined with GSH to form a complex. As the reaction with glutathione proceeds, the fluorescence intensity of AuNCs decreases, and the catalytic ability increases. Subsequently, the staphylococcal enterotoxin aptamer was immobilized on the ESM membrane. During the detection process, due to the combination of staphylococcal enterotoxin and its aptamer to form a complex, the catalytic site of AuNCs was masked. At this time, the chromogenic enzyme substrate was added, and the color changed. According to the color change, a colorimetric method for rapid detection of staphylococcal enterotoxin was established, which opened up a new method for food safety detection [45] (Figure 4).

2.1.4 Lysozyme

Lysozyme is an antibacterial enzyme widely found in bacteria, fungi, animals, and plants. Their main function is to destroy bacterial cell walls by hydrolyzing the β-1,4-glycosidic bond between *N*-acetylglucosamine and *N*-acetylmuramic acid in peptidoglycan chains. Lysozyme has many excellent properties, such as acid and alkali resistance, strong thermal stability, and excellent antibacterial performance [46]. Egg whites are the main source of lysozyme. However, other sources, including tears, saliva, plasma, mucus, and skin, are also good sources of lysozyme, which can also be found in some plants. Lysozyme was first used in 2010 to replace BSA as a template for synthesizing protein-AuNCs [47]. The synthesized lysozyme-AuNCs exhibited a strong fluorescence emission at approximately 650 nm, with a QY of 5.6%. Transmission electron microscopy (TEM) has confirmed that the formed lysozyme-AuNCs were spherical with a particle size of approximately 1 nm. In the same year, Lin and Tseng conducted similar experiments to synthesize fluorescent AuNCs using lysozyme VI as the template [48]. The excitation and emission wavelengths were 400 and 631 nm, respectively. The molecular weight determined by MALDI-TOF mass spectrometry was 5 kDa. In terms of potential applications, lysozyme VI-AuNCs improved the detection of Hg^{2+} by approximately 330 times compared to its previous value. The detection limits for CH_3Hg^+ and Hg^{2+} were 4 pM and 3 nM, respectively. Subsequent studies used lysozyme VI under acidic conditions to synthesize highly fluorescent AuNCs [49]. These new lysozyme VI-AuNCs emitted blue fluorescence at 455 nm upon excitation at 380 nm with a considerably high QY of 56%. The authors investigated the differences between the lysozyme VI-AuNCs synthesized at different pH levels by studying their growth mechanisms. At pH 3, the conformation of lysozyme type VI is more compact, therefore, a smaller template for the synthesis of AuNCs. This leads to

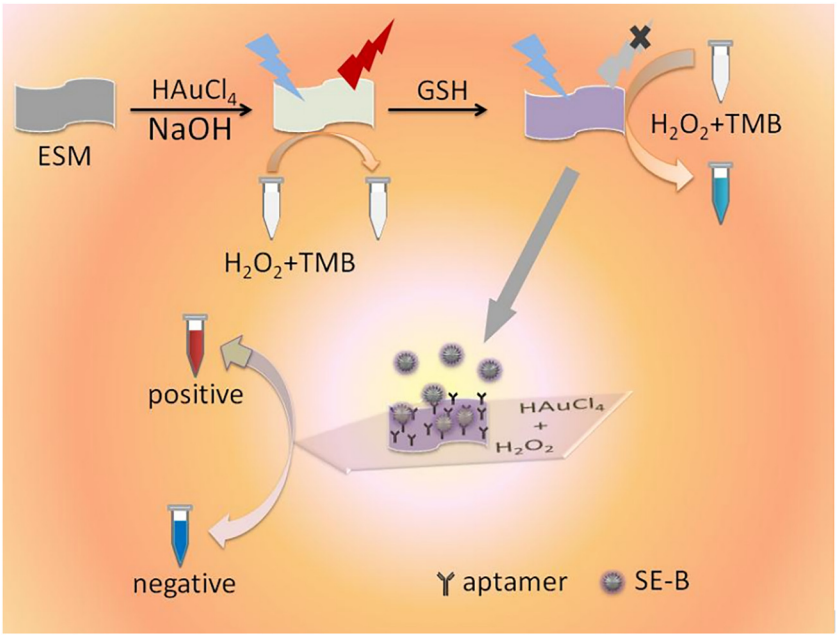

Figure 4: Schematic diagram of AuNCs synthesized by Eggshell membrane.

lysozyme VI-AuNCs with a high QY. Comparatively, high pH values led to the denaturation of lysozyme type VI, resulting in a lower QY. A study demonstrated that functional lysozyme-AuNCs could act as antibacterial agents against drug-resistant bacteria [50]. When excited at 395 nm, the synthesized lysozyme-AuNCs exhibited a strong red fluorescence emission at 640 nm. The QY was 3.6 ± 0.4%, and the TEM image showed that the size of the synthesized lysozyme-AuNCs was approximately 2.3 ± 0.3 nm. The characterization results of inductively coupled plasma mass spectrometry and FTIR showed that almost 100 lysozyme molecules were present in a single AuNC. Furthermore, the authors also observed that lysozyme-AuNCs showed high stability in extremely alkaline and high salt concentration solutions. Subsequently, the prepared lysozyme-AuNCs were used as fluorescent labels and antibacterial sensors for microorganisms. The results showed that the nanoclusters inhibited the growth of drug-resistant bacteria owing to the absence of cysteine residues in lysozyme; therefore, the activity of lysozyme-AuNCs was not affected by Au–S binding. In addition, lysozyme-AuNCs were used as fluorescent probes to detect cyanide anions [51] (Figure 5).

2.1.5 Trypsin

Trypsin is a serine proteolytic enzyme that acts mainly as a digestive enzyme in vertebrates. It is the most specific protease to achieve the function of hydrolyzing protein by breaking lysine or arginine carboxyl group [52]. In 2011, trypsin was first used to synthesize AuNCs, and fluorescent trypsin-AuNCs with a red emission wavelength of 640 nm were synthesized in an alkaline aqueous solution. The authors found that its photostability was similar to that of cadmium selenide quantum dots and that mercury ions could specifically quench its fluorescence. The authors used this feature to detect mercury ions sensitively and selectively with a detection limit of 50–10 nM [53]. Subsequently, trypsin-AuNCs synthesized by researchers emitted red fluorescence at 645 nm when excited at 360 nm, and TEM images revealed that they had a diameter of approximately 2 nm. MALDI-TOF mass spectrometry results showed that the molecular weight of the trypsin-AuNCs was 5 kDa and that they had a QY of 6.5% [12]. The authors designed a biosensor based on surface plasmon-enhanced cysteamine-gold nanoparticles and trypsin-AuNCs for the detection of heparin and *in vivo* cancer cell imaging. Heparin-guided energy transfer between trypsin-AuNCs and cysteamine-modified nanogold was used to generate the signal output of the fluorescent biosensor. The linear range of the biosensor was 0.1–4.0 μg/mL, and the heparin detection limit was 0.05 μg/mL. *In vivo* studies in mice have used folic acid to modify trypsin-AuNCs. This modified folic acid-trypsin-AuNC probe had high specificity for detecting HeLa tumors (Figure 6).

2.1.6 Pepsin

Pepsin was first discovered in the early nineteenth century and was the first enzyme found in animals. Pepsin is a gastric aspartic protease with a molecular weight of

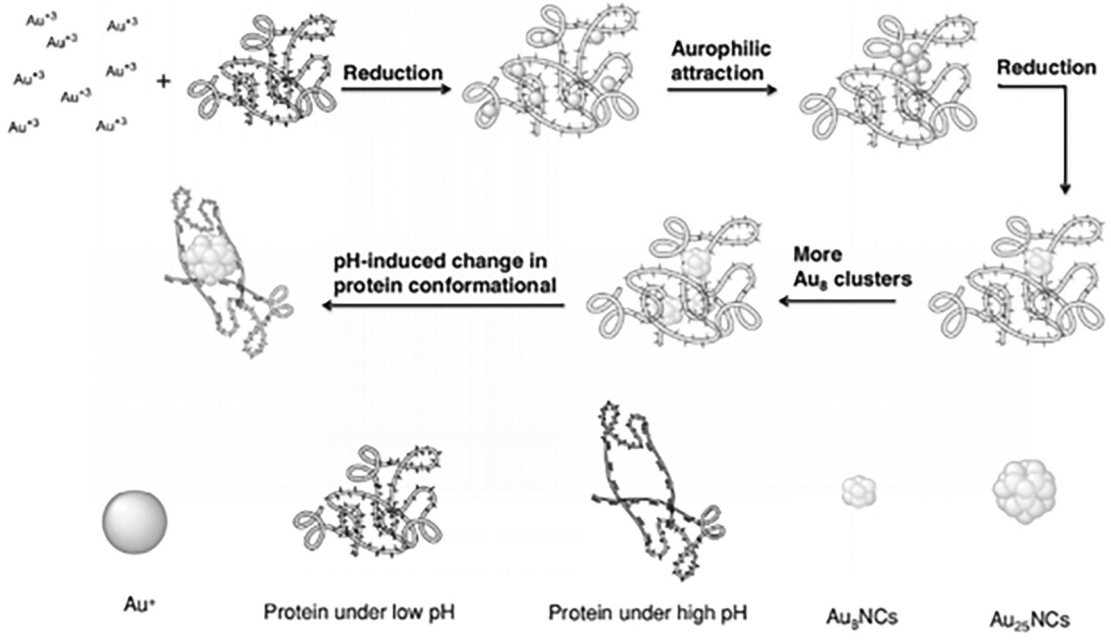

Figure 5: Schematic diagram of AuNCs synthesized by lysozyme.

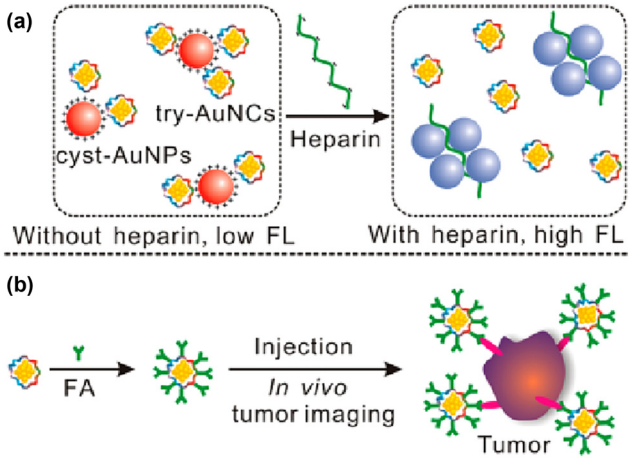

Figure 6: (a) Schematic diagram of the selective detection of heparin for energy transfer between surface plasma-enhanced Cyst-AuNPs and Try-AuNCs. (b) Schematic diagram of folic acid-modified Try-AuNCs for *in vivo* cancer imaging.

approximately 3.4 kDa. The main site of pepsin hydrolysis is the peptide bond formed by the amino groups of aromatic amino acids or acidic amino acids. Pepsin plays an important role in digestion in vertebrates [54]. A team conducted a study and prepared pepsin-AuNCs with blue, green, and red fluorescence emissions at different pH conditions [55]. Among them, Au_{25}NCs (pH = 12) emitted red fluorescence at 670 nm, which was similar to the results of previous studies. Au_{13}NCs (pH = 1) emitted green fluorescence at 510 nm. Au_8NCs and Au_5NCs (pH = 9) emitted blue fluorescence at 480 and 402 nm, respectively. The QY of the red-, green-, and blue-emitting AuNCs were 3.5, 5.0, and 3.7%, respectively. XPS proved that the binding energy of the pepsin-AuNCs increased with decreasing particle size. The authors hypothesized that the red-fluorescent Au_{25}NCs were stabilized by weakly bonded random helical pepsin and that the alkaline synthesis conditions used led to the denaturation of the peptide-protein in the internal space of the enzyme, which resulted in a larger space to bind more gold atoms. At low pH (less than 1), pepsin autolysis occurs, and the smaller internal space produced by the early hydrolysate may act as a template to produce smaller Au_{13}NCs. In the pH range of 3–6, different forms of AuNCs were formed, including gold nanoplates with sizes of hundreds of nanometers (Figure 7).

An increasing number of animal-derived proteins are being used to prepare protein-AuNCs. For example, researchers have used immunoglobulins to prepare and functionalize AuNCs. The prepared immunoglobulin-AuNCs can emit strong red

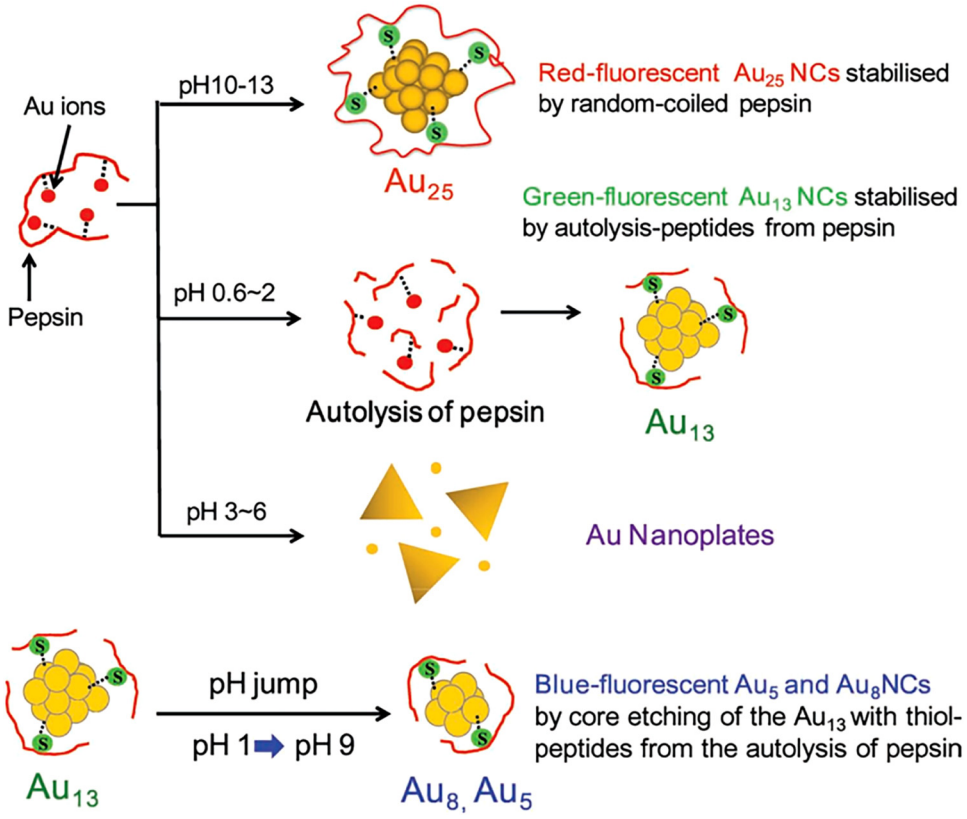

Figure 7: Schematic diagram of AuNCs synthesized by pepsin under different pH.

fluorescence and have high photoluminescence QY [56]. It retains the biological activity of immunoglobulins and enables them to bind to goat anti-human immunoglobulins. The authors developed a simple detection method based on a fluorescence-labeled dot immunoassay that has considerable potential for the development of efficient biosensors. Other researchers used protamine as a template for preparing AuNCs. The authors found that 1-hydroxypyrene could induce the aggregation of AuNCs through hydrogen bonding and electrostatic and hydrophobic interactions, resulting in the enhancement of the photoluminescence of the protamine-AuNCs [57]. Based on this feature, a highly sensitive and selective quantitative strategy for the detection of 1-hydroxypyrene was proposed.

2.2 Plant-derived proteins

Plant-derived proteins such as soybean protein, pea protein, papain, horseradish peroxidase (HRP), and lysozyme also play important roles in the preparation of AuNCs because of their unique physical and chemical properties and spatial structure.

2.2.1 HRP

HRPs, which are present in horseradish plants, have been widely studied for over half a century and are members of the peroxidase family. In 1976, Welinder identified the first complete amino acid sequence of HRP [58]. It contains numerous isozymes. HRP C is the most common member of the plant peroxidase superfamily and is one of the most thoroughly studied members [59]. HRP contains 308 amino acid residues and is rich in tyrosine and cysteine residues. The three-dimensional structure of HRP consists of two domains, the proximal and distal domains, with a heme group located between them. Its amino acid composition and unique three-dimensional structure make it an ideal template for AuNC synthesis. In 2011, for the first time, HRP-AuNCs were greenly synthesized under physiological conditions using HRP as a template [60]. The HRP-AuNCs synthesized by this method not only retain the catalytic function of the enzyme but also exhibit the fluorescence characteristics of AuNCs. The catalytic activity of HRP is well preserved. The addition of hydrogen peroxide quantitatively quenched the fluorescence of the HRP-AuNCs, and it was assessed for hydrogen peroxide detection applications. Recently, an HRP-encapsulated fluorescent bionanomaterial consisting of BSA-stabilized AuNCs and HRP-stabilized AuNCs was reported [61]. The material exhibited a two-step fluorescence quenching effect. Based on this effect, the author designed a device for the detection of hydrogen peroxide. The detection limit was as low as 0.5 nM, which could be detected by the naked eye and had good selectivity. This device can be used to detect other substances and enzymes that produce hydrogen peroxide (Figure 8).

2.2.2 Papain

Papain is a cysteine protease, also known as papaya protease, extracted from papaya and has the advantages of low price and easy access. Papain can decompose proteins through amide bond cleavage in acidic, neutral, and alkaline environments and has a wide substrate specificity. It

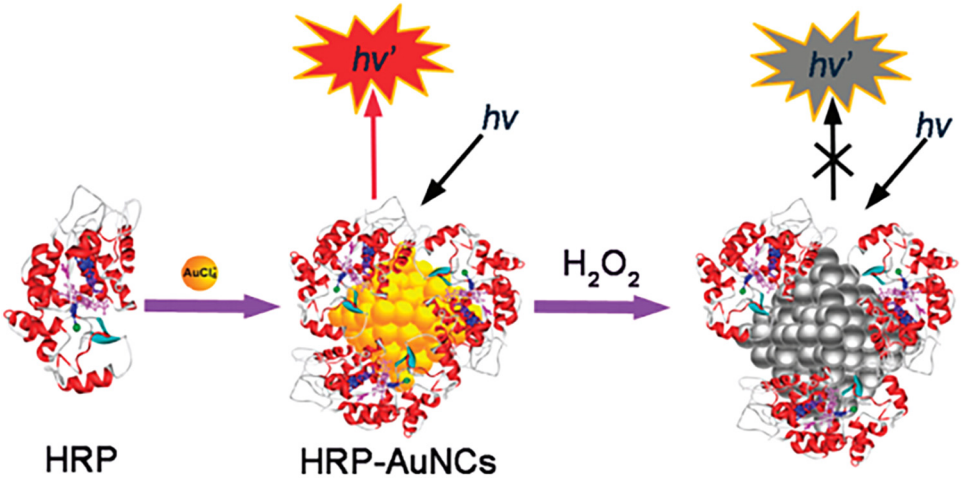

Figure 8: Schematic diagram of AuNCs synthesized by HRP.

acts on the peptide bonds formed by L-arginine, L-lysine, and L-papain amino acid residue carboxyl groups in the protein. Papain can break down proteins into small fragments; therefore, it is often used in food manufacturing, such as meat processing, or as a stabilizer for brewing [62]. In 2013, papain was first used as a template to synthesize highly fluorescent papain-AuNCs under alkaline conditions [63]. The synthesized papain-AuNCs produced red fluorescence emission at 660 nm and had a QY of 4.3%. Meanwhile, the average particle size of the clusters was 1.2 ± 0.2 nm. In previous studies, 35 cysteine residues in BSA were involved in the formation of BSA-AuNCs. However, papain only contains eight cysteines. The authors speculate that in addition to cysteine residues, other amino acid residues may be involved in the synthesis and growth of AuNCs. Changes in the secondary structure of papain were observed using FTIR and circular dichroism spectroscopy, which confirmed the theory. Compared to BSA, the spectral changes in papain were more obvious, and BSA has more thiol groups than papain. In previous studies, thiol groups have been considered to play an important role in the formation of AuNCs. The fluorescence emission of the synthesized papain-AuNCs is considerably stable at room temperature for over 3 months, making it an ideal biostable fluorescent sensor. The fluorescent probe exhibits high sensitivity and selectivity for the determination of Cu^{2+} by fluorescence quenching, and the Cu^{2+} detection limit is 3 nM. Subsequently, researchers used papain to produce fluorescent papain-AuNCs. D-Penicillamine restored the fluorescence quenching caused by Cu^{2+}. To understand this mechanism, a set of quantitative detection methods for D-penicillamine was developed [64]. The papain-AuNCs synthesized produced red fluorescence emission at 639 nm and had an average size of approximately 5.7 nm. Owing to the bonding of Cu^{2+} and papain amino acid residues on the surface of the papain-AuNCs, the nanoclusters exhibited high selectivity and sensitivity to Cu^{2+}. In this study, D-penicillamine was added to the papain-AuNC-Cu^{2+} complex, the fluorescence quenched by Cu^{2+} was immediately restored, and the papain-AuNC was found to detect D-penicillamine in real samples with a detection limit of 5.0 mM. Compared with the previous D-penicillamine detection technology [65], this method is not only a green and harmless process. The experimental operation is simple, and the detection is sensitive and selective. In the same year, another researcher invented a one-pot method to generate fluorescent AuNCs using papaya juice as a reducing agent [66]. The prepared papaya juice-AuNCs exhibited green fluorescence emission, and TEM showed that the average size was 6.9 nm. Furthermore, it was found that the fluorescence of papaya juice-AuNCs remained stable for at least 2 months. A papaya juice-AuNC fluorescent probe was used to monitor L-lysine in biological samples, and the detection limit was 6.0 μM. The reaction time was very short, only 120°C reaction for 3 min, thereby achieving the effect of rapid detection. Glyphosate is the most widely used herbicide in the world, and as such, papain was used to prepare AuNCs that showed specific fluorescence quenching for glyphosate and had a QY of 12.4%. Visual or semiquantitative glyphosate detection was performed. In a real sample detection experiment, the sample recovery rate was between 97.3 and 118%, indicating that this detection method has considerable potential for practical applications [67] (Figure 9).

2.2.3 Soybean protein

Soybeans are a good source of plant protein. Approximately 90% of soybean protein consists of β-conglycinin and glycinin [68]. β-Conglycinin is a trimeric glycoprotein composed of three subunits with a molecular weight of 150–200 kDa. It is rich in content and exhibits strong thermal stability. Soybean globulin is a hexamer with a molecular weight of 300–380 kDa. Researchers have synthesized gold nanomaterials of different shapes and sizes using soybean protein isolate as the precursor [69]. For example, soybean protein isolate induced the

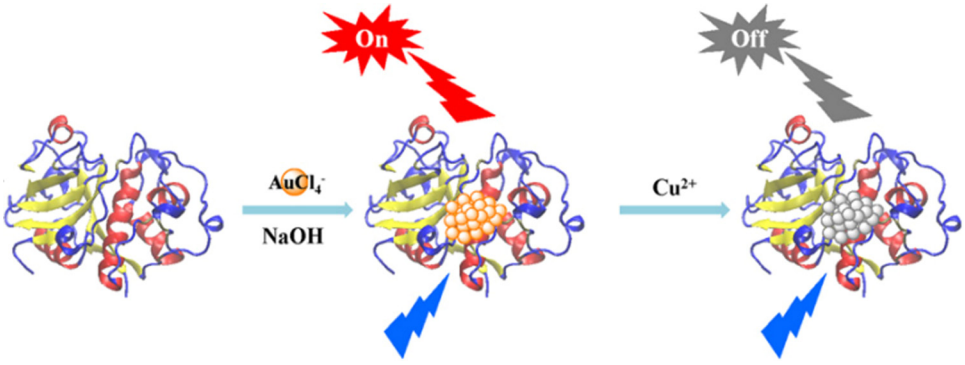

Figure 9: Schematic diagram of AuNCs synthesized by papain.

Figure 10: Schematic diagram of AuNCs synthesized by soy protein.

formation of gold nanosheets under acidic pH conditions. Meanwhile, at alkaline pH levels, the gold ions captured by the protein are gradually reduced to form AuNCs. The particle size range of soybean protein-AuNCs is 1.3–4.9 nm, and the average particle size is 2.6 nm. The authors believe that the formation of AuNPs during long-term alkaline incubation may be due to the degradation of soybean protein isolate. The degradation of the protein means that its structure cannot couple to larger nanosheets to form nanoparticles. The control experiments conducted in this study have revealed that soybean protein-AuNCs are only stable when synthesized with globular proteins, whereas fibrillin can induce gold ions to form gold nanoparticles but cannot be used as a template for the synthesis of protein-AuNCs. Fluorescence spectroscopy, circular dichroism, and Fourier transform infrared spectroscopy have been used to study and analyze the relationship between

Table 1: Proteins used to synthesize protein-AuNCs

Protein	Reaction condition	Size (nm)	Optical property	Application	Ref.
BSA	37°C, 12 h	2	QY: 3.5%	Phototheranostics of cancer and bacterial infections	[73]
BSA	37°C, 12 h	2.47 ± 0.42	365/690 nm (Ex/Em)	Detection of heavy metal ions	[74]
BSA	37°C, 12 h	3	495/675 nm (Ex/Em)	Detection of cysteine and Cu^{2+}	[75]
BSA	37°C, 12 h	1.3	405/680 nm (Ex/Em)	ROS and singlet oxygen generation	[76]
BSA	37°C, 12 h		385/650 nm (Ex/Em)	Detection of trypsin	[22]
BSA	37°C, 12 h	1–3	365/650 nm (Ex/Em)	Detection of Quercetin flavonoids	[77]
BSA	37°C	1.5	385/650 nm (Ex/Em)	Detection of total antioxidant capacity	[78]
BSA	37°C, 12 h	1.95	QY: 6% 370/610 nm (Ex/Em)	Detection of alkaline phosphatase	[79]
BSA	37°C, 12 h	2.75	360/650 nm (Ex/Em)	Detection Hg^{2+} with pyridoxal modification	[80]
BSA	37°C, 24 h	2–3	530/670 nm (Ex/Em)	Fluorescent contrast agents for cellular	[81]
CEW	37°C, 12 h	2–3	470/630 nm (Ex/Em)	Detection of organophosphorus pesticides	[82]
CEW	90 W, microwave heating	2.6 ± 0.5	370/640 nm (Ex/Em)	Detection of phosphate containing metabolites	[40]
CEW	37°C, 20 h	2–3	360/640 nm (Ex/Em)	Determining prooxidant activities	[83]
CEW	90 W, microwave heating	3.57 ± 0.56	365/667 nm (Ex/Em)	Detection of Hg^{2+}	[84]
Lysozyme	37°C, 12 h	1–2	380/666 nm (Ex/Em)	Detection of cyanide	[85]
Lysozyme	37°C, 24 h	3		Therapy of osteoporosis	[86]
Lysozyme	50°C, microwave heating, 5 min	1.73 ± 0.0035	380/650 nm (Ex/Em)	Detection of folic acid and bioimaging	[87]
Lysozyme	37°C, 12 h	2.97	365/665 nm (Ex/Em)	Detection of Zn^{2+}	[88]
Trypsin		5.2 ± 1	QY: 7.9% 520/665 nm (Ex/Em)	Detection of carbidopa, dopamine, Cu^{2+}, Co^{2+} and Hg^{2+}	[89]
Trypsin	37°C, 12 h	2.8	365/625 nm (Ex/Em)	Detection of sulfide	[90]
HSA	37°C, 12 h	2	474/609 nm (Ex/Em)	NIR laser-mediated treatment	[91]
HSA	300 W, microwave heating, 6 min	2.5	370 nm, 500 nm/645 nm (Ex/Em)	Detection of free bilirubin sensitively in serum samples	[92]
β-Lactoglobulin	37°C, 2–3 h	2–10	510/650 nm (Ex/Em)	Detection of Hg^{2+}/Cell and animal imaging	[93]
Pepsin	RT, 3 h	2	416/655 nm (Ex/Em)	"Turn-off" detection of spermine	[94]
HRP	37°C, 12 h	1–2	365/630 nm (Ex/Em)	Electrochemical sensing, detection of H_2O_2	[95]
Papain	37°C, 6 h	3	470/650 nm (Ex/Em)	Detection of sulfide ions	[96]
Gluten protein	50°C, 1 h	2.78	370/640 nm (Ex/Em)	Detection of Hg^{2+}	[97]
Glutenin	37°C, 5 h	2.3 ± 0.7	370/610 nm (Ex/Em)	Detection of vitamin B1	[98]

the fluorescence changes of soybean protein-AuNCs and the conformational changes in soybean protein ligands during the AuNCs synthesis [13]. According to the fluorescence spectrum analysis, the fluorescence peak intensity before the reaction had taken place was mainly due to the gold core. However, after the reaction had taken place, it was determined that the fluorescence peak intensity was due to a combination of the gold core and the protein-ligand. Circular dichroism and Fourier-transform infrared spectroscopy revealed that the conformation of the soybean protein-ligand changed significantly with increasing reaction time. The structure of the soybean protein changed from ordered to disordered and then to ordered. This proved that the main driving force behind the reaction was to protect the gold nucleus and transfer electrons from the ligand to the gold ion, thereby affecting its fluorescence emission. AuNCs synthesized from soy proteins were used for the detection of bismerthiazol. Bismerthiazol is a fungicide that is used to control bacterial infections in plants, particularly during rice cultivation. Thiadiazole can cause chronic oral toxicity and thyroid damage in rats and may cause similar problems in humans [70]. Currently, high-performance liquid chromatography is used to assess the bismerthiazol content. But there is a need for a quick, simple, and sensitive method with which to improve bismerthiazol sensing [71]. As such, soybean protein-AuNCs were used to develop a method for the rapid and sensitive detection of bismerthiazol in Chinese cabbage [58]. In this experiment, soybean protein was extracted by acid precipitation and alkali extraction before soybean protein-AuNCs were synthesized after freeze-drying. The soybean protein-AuNCs exhibited strong pink fluorescence emission at 600 nm, and their average size was 3 nm. The authors observed that the fluorescence of the clusters was quenched by thiazole. It was postulated that this was due to the presence of two sulfhydryl groups in thiazole that can quench the fluorescence of AuNCs by forming sulfates and metal complexes (Figure 10).

In addition to the aforementioned plant-derived proteins, several researchers have attempted to synthesize AuNCs and apply them in various directions. For example, some researchers have used pea protein to prepare AuNCs with strong red fluorescence, which are stable for up to one month. The pea protein-AuNCs were investigated for their potential in tumor cell imaging [72] (Table 1).

3 Conclusion

In recent decades, science and technology based on nanomaterials have attracted significant interest and undergone rapid development. An increasing number of excellent nanomaterials have been developed for various potential applications [2,99]. Biological components play important roles in the development of nanomaterials owing to their unique characteristics and excellent properties. For example, zinc oxide nanoflowers were synthesized using four ginseng extracts and used the nanoflowers as efficient photocatalysts to degrade industrial dyes under ultraviolet irradiation [100]. Meanwhile, silver nanoparticles have been synthesized using *Nigella sativa* seed-cake extracts. The synthesized nanoparticles exhibited good stability and high antibacterial activity against *Staphylococcus aureus*, *Bacillus subtilis*, *Pseudomonas aeruginosa*, and *Escherichia coli* [101]. Furthermore, magnetic Fe_3O_4 nanoparticles were synthesized using *Garcinia mangostana* fruit peel extract as a stabilizer. The compounds were tested for their cytotoxicity, while their potential applications to hyperthermia therapy and anticancer treatments were explored [102]. High-fluorescence carbon quantum dots were synthesized using a hydrothermal method with aloe as the carbon source, which emitted bright yellow photoluminescence. The selective detection of xylazine in food samples could be achieved by static quenching using the quantum dots [103]. Another study reported the synthesis of orange fluorescent AuNCs using turmeric root extract and 11-mercaptoundecanoic acid as the reducing agent and capping ligand, respectively. The prepared AuNC had a high QY of 8.4% and could independently and specifically detect cadmium, zinc, and copper ions [104].

As important representatives of nanomaterials, researchers are no longer satisfied with traditional AuNPs. AuNCs, one of the emerging nanomaterials, have been discovered and studied for more than 10 years. Protein synthesis of fluorescent protein-AuNCs is a promising research direction and has attracted considerable attention. Numerous proteins extracted from common food items such as eggs, milk, meat, and fruits have been used to prepare fluorescent and biocompatible AuNCs. Protein templates provide important support for AuNC formation. This article reviews the synthesis and related applications of AuNCs synthesized from natural proteins. The advantage of using proteins in the synthesis of AuNCs is that functional amino acids can be sensitively activated to capture bound gold ions. Meanwhile, the unique spatial structure of protein shells creates many suitable sites for the formation of AuNCs. These novel protein-stabilized protein-AuNCs play an increasingly important role in the detection of heavy metal ions, bioactive nutrients, and biomolecules. The protein-AuNCs are able to do so because of their extraordinary physical and chemical properties, including their ultrasmall size, fluorescence, and good biocompatibility. In addition, these protein-AuNCs can be used as biological probes or contrast agents.

Natural protein-templated AuNCs are environmentally friendly, easy to obtain, and easy to prepare under mild conditions, with good biocompatibility and light stability. These functions have gradually been applied in the fields of rapid detection and biological imaging applications. Although many detailed studies have been conducted, there is still considerable scope for development in this research field.

First, the mechanism of protein-templated synthesis of AuNCs remains unclear. Extensive attempts to synthesize natural proteins will help discover excellent synthesis methods and summarize the methods and experience of synthesis. For example, most existing methods fail to produce protein-AuNCs of uniform size and distribution. Meanwhile, strongly acidic or alkaline conditions are not conducive to maintaining the natural structure of the template protein. These imperfections seriously affect the properties of protein-AuNCs and lead to the loss of the biological activity of the protein. Therefore, mild approaches for the synthesis, separation, and purification of protein-AuNCs are required. While the techniques that can control the size and morphological distribution of protein-AuNCs are desirable. To achieve this, the mechanism of protein-AuNCs synthesis needs to be elucidated and understood. Few studies have explored the structural relationship between proteins and gold ions, such as the positions of AuNCs and how proteins are combined and stabilized. This important structural information will enable a better understanding of the evolution of fluorescent protein-AuNCs during synthesis and provide a deep understanding of their structures and functions. More detailed structural information will promote further progress and breakthroughs in the synthesis and applications of fluorescent protein-AuNCs, such as the influence of pH on the structural and conformational changes of protein. In most synthesis methods, the pH of the synthetic environment is adjusted to alkaline conditions. The common explanation given by researchers is that under alkaline conditions, the protein conformation will change from folded to unfolded. In the process, the spatial protein structure will become larger, and more gold binding sites will be exposed, which facilitates the formation of protein-AuNCs. This trend was observed when pepsin-AuNCs were synthesized at different pH levels, and the higher the pH, the larger the synthesized pepsin-AuNCs were. In future in-depth studies, it is feasible to systematically study the influence of protein structure change information on the synthesis of AuNCs under different pH conditions, such as whether there are changes in binding sites, the time required for synthesis, fluorescence emission changes, AuNCs' size, and so on.

Second, the QY of natural protein-AuNCs remains low (most are less than 10%). A method was developed to improve the brightness and stability of BSA-AuNCs by covalently combining sulfided-gold clusters with BSA-AuNCs *via* carbodiimide activation coupling [105]. It was found that the formation of a polymer-like protective layer around the gold core played a crucial role in this improvement. Therefore, protein modification may be a feasible way to synthesize AuNCs with strong fluorescence, high QY, and high stability. The QY of bimetallic nanoclusters is higher than those of AuNCs [106]. Bimetallic gold and silver alloy nanoclusters with BSA as the template were synthesized using a one-pot method [107]. The prepared gold-silver alloy nanoclusters exhibited an obvious red fluorescence enhancement, which was approximately 6.5 times higher than that of ordinary BSA-AuNCs.

Third, the current applications mainly focus on detection and bioimaging. The main characteristics of protein-templated AuNCs are their stability, biocompatibility, and environmental friendliness. At present, the main advantage and characteristic of AuNCs synthesized using natural proteins is their biological activity, which further expands the application of AuNCs [20]. We believe that more applications can be achieved through the biological activities of natural proteins. For example, researchers have used HRP as a template to synthesize fluorescent AuNCs and observed that the fluorescence of the HRP-AuNCs completely disappeared after the addition of hydrogen peroxide [60]. This is because horseradish retains its biological activity after synthesis and maintains its basic catalytic function in the decomposition of hydrogen peroxide. A variety of proteins in animals and plants play important roles in the biological, medical, food, and chemical industries. Protein-AuNCs have abundant resources [108]. However, not all proteins can be used to synthesize AuNCs, and the synthesized AuNCs must retain the function of some proteins while maintaining high stability and QY. Therefore, researchers need to screen proteins for synthesis, accompanied by subsequent improvements, to promote the role of AuNCs in industrial, biological, medical, and analytical fields.

Over the past few decades, significant progress has been made in the field of protein-guided fluorescent AuNCs. There are several challenges to overcome, and more work needs to be conducted. With progress in synthetic methods and related structural analyses, it is believed that these new nanoclusters will have more applications in food detection, environmental monitoring, biomarkers, bioimaging, and disease diagnosis.

Funding information: This project was supported by the National Natural Science Foundation of China (Project No: 32060224) and the Shihezi University Innovation Development Project (Project No: CXFZ202110) for the publication of this article.

Author contributions: All authors have accepted responsibility for the entire content of this manuscript and approved its submission.

Conflict of interest: The authors state no conflict of interest.

References

[1] Mansoori GA, Soelaiman TF. Nanotechnology–An introduction for the standards community. West Conshohocken, PA, USA: ASTM International; 2005.

[2] Bayda S, Adeel M, Tuccinardi T, Cordani M, Rizzolio F. The history of nanoscience and nanotechnology: From chemical-physical applications to nanomedicine. Molecules. 2019;25(1):112. doi: 10.3390/molecules25010112.

[3] Lin Y, Ren J, Qu X. Nano-gold as artificial enzymes: Hidden talents. Adv Mater. 2014;26(25):4200–17. doi: 10.1002/adma.201400238. Shakeri-Zadeh A, Zareyi H, Sheervalilou R, Laurent S, Ghaznavi H, Samadian H. Gold nanoparticle-mediated bubbles in cancer nanotechnology. J Control Release. 2021;330:49–60. 10.1016/j.jconrel.2020.12.022.

[4] Mo F, Zhou Q, He Y. Nano-Ag: Environmental applications and perspectives. Sci Total Environ. 2022;829:154644; doi: 10.1016/j.scitotenv.2022.154644; McGillicuddy E, Murray I, Kavanagh S, Morrison L, Fogarty A, Cormican M, et al. Silver nanoparticles in the environment: Sources, detection and ecotoxicology. Sci Total Environ. 2017;575:231–46. 10.1016/j.scitotenv.2016.10.041.

[5] Wang Z, Liang K, Chan SW, Tang Y. Fabrication of nano CuAl(2)O(4) spinel for copper stabilization and antibacterial application. J Hazard Mater. 2019;371:550–7. doi: 10.1016/j.jhazmat.2019.02.053.

[6] Mu J, Li C, Shi Y, Liu G, Zou J, Zhang DY, et al. Protective effect of platinum nano-antioxidant and nitric oxide against hepatic ischemia-reperfusion injury. Nat Commun. 2022;13(1):2513. doi: 10.1038/s41467-022-29772-w.

[7] Aiken JD, Finke RG. A review of modern transition-metal nanoclusters: their synthesis, characterization, and applications in catalysis. J Mol Catal A-Chem. 1999;145(1–2):1–44. doi: 10.1016/s1381-1169(99)00098-9.

[8] Zhang B, Chen J, Cao Y, Chai OJH, Xie J. Ligand design in ligand-protected gold nanoclusters. Small. 2021;17(27):e2004381. doi: 10.1002/smll.202004381.

[9] Cordon J, Jimenez-Oses G, Lopez-de-Luzuriaga JM, Monge M. The key role of Au-substrate interactions in catalytic gold subnanoclusters. Nat Commun. 2017;8(1):1657. doi: 10.1038/s41467-017-01675-1.

[10] Thompson D, Hermes JP, Quinn AJ, Mayor M. Scanning the potential energy surface for synthesis of dendrimer-wrapped gold clusters: Design rules for true single-molecule nanostructures. ACS Nano. 2012;6(4):3007–17. doi: 10.1021/nn204470g.

[11] Liao L, Wang C, Zhuang S, Yan N, Zhao Y, Yang Y, et al. An unprecedented Kernel growth mode and layer-number-odevity-dependent properties in gold nanoclusters. Angew Chem Int Ed Engl. 2020;59(2):731–4. doi: 10.1002/anie.201912090. Chai OJH, Wu Z, Xie J. All hydroxyl-thiol-protected gold nanoclusters with near-neutral surface charge. J Phys Chem Lett. 2021;12(40):9882–7. 10.1021/acs.jpclett.1c02989.

[12] Liu JM, Chen JT, Yan XP. Near infrared fluorescent trypsin stabilized gold nanoclusters as surface plasmon enhanced energy transfer biosensor and *in vivo* cancer imaging bioprobe. Anal Chem. 2013;85(6):3238–45. doi: 10.1021/ac303603f.

[13] Cheng Y, Chen J, Hu B, Pi F, Yu H, Guo Y, et al. Spectroscopic investigations of the changes in ligand conformation during the synthesis of soy protein-templated fluorescent gold nanoclusters. Spectrochim Acta A Mol Biomol Spectrosc. 2021;255:119725. doi: 10.1016/j.saa.2021.119725.

[14] Borse S, Murthy ZVP, Kailasa SK. Synthesis of gold and copper bimetallic nanoclusters with papain for fluorescence detection of cortisone in biological samples. Anal Bioanal Chem. 2023;415(2):335–43. doi: 10.1007/s00216-022-04412-w.

[15] Zhao P, Liu S, Wang L, Liu G, Cheng Y, Lin M, et al. Alginate mediated functional aggregation of gold nanoclusters for systemic photothermal therapy and efficient renal clearance. Carbohydr Polym. 2020;241:116344. doi: 10.1016/j.carbpol.2020.116344.

[16] Yadav A, Verma NC, Rao C, Mishra PM, Jaiswal A, Nandi CK. Bovine serum albumin-conjugated red emissive gold nanocluster as a fluorescent nanoprobe for super-resolution microscopy. J Phys Chem Lett. 2020;11(14):5741–8.

[17] Xia X, Long Y, Wang J. Glucose oxidase-functionalized fluorescent gold nanoclusters as probes for glucose. Anal Chim Acta. 2013;772:81–6. doi: 10.1016/j.aca.2013.02.025.

[18] Griep MH, Sellers MS, Subhash B, Fakner AM, West AL, Bedford NM. Towards the identification of the gold binding region within trypsin stabilized nanoclusters using microwave synthesis routes. Nanoscale. 2021;13(2):1061–8. doi: 10.1039/d0nr07068h.

[19] Li C, Chen H, Chen B, Zhao G. Highly fluorescent gold nanoclusters stabilized by food proteins: From preparation to application in detection of food contaminants and bioactive nutrients. Crit Rev Food Sci Nutr. 2018;58(5):689–99. doi: 10.1080/10408398.2016.1213698.

[20] Li Y, Cao Y, Wei L, Wang J, Zhang M, Yang X, et al. The assembly of protein-templated gold nanoclusters for enhanced fluorescence emission and multifunctional applications. Acta Biomater. 2020;101:436–43. doi: 10.1016/j.actbio.2019.10.035.

[21] Lillo CR, Calienni MN, Rivas Aiello B, Prieto MJ, Rodriguez Sartori D, Tuninetti J, et al. BSA-capped gold nanoclusters as potential theragnostic for skin diseases: Photoactivation, skin penetration, in vitro, and *in vivo* toxicity. Mater Sci Eng C Mater Biol Appl. 2020;112:110891. doi: 10.1016/j.msec.2020.110891. Zhang XD, Wu D, Shen X, Liu PX, Fan FY, Fan SJ. *In vivo* renal clearance, biodistribution, toxicity of gold nanoclusters. Biomaterials. 2012;33(18):4628–38. 10.1016/j.biomaterials.2012.03.020.

[22] Hu L, Han S, Parveen S, Yuan Y, Zhang L, Xu G. Highly sensitive fluorescent detection of trypsin based on BSA-stabilized gold nanoclusters. Biosens Bioelectron. 2012;32(1):297–9. doi: 10.1016/j.bios.2011.12.007.

[23] Chevrier DM, Chatt A, Zhang P. Properties and applications of protein-stabilized fluorescent gold nanoclusters: short review. J Nanophotonics. 2012;6(1):064504.

[24] Zivkovic AM, Barile D. Bovine milk as a source of functional oligosaccharides for improving human health. Adv Nutr. 2011;2(3):284–9. doi: 10.3945/an.111.000455.

[25] Ding C, Xu Y, Zhao Y, Zhong H, Luo X. Fabrication of BSA@AuNC-based nanostructures for cell fluoresce imaging and target drug

delivery. ACS Appl Mater Interfaces. 2018;10(10):8947–54. doi: 10.1021/acsami.7b18493.
[26] Willett R, Baldwin K, West K, Pfeiffer L. Differential adhesion of amino acids to inorganic surfaces. Proc Natl Acad Sci. 2005;102(22):7817–22.
[27] Xie J, Zheng Y, Ying JY. Protein-directed synthesis of highly fluorescent gold nanoclusters. J Am Chem Soc. 2009;131(3):888–9.
[28] Wen X, Yu P, Toh Y-R, Tang J. Structure-correlated dual fluorescent bands in BSA-protected Au25 nanoclusters. J Phys Chem C. 2012;116(21):11830–6. doi: 10.1021/jp303530h.
[29] Le Guével X, Hötzer B, Jung G, Hollemeyer K, Trouillet V, Schneider M. Formation of fluorescent metal (Au, Ag) nanoclusters capped in bovine serum albumin followed by fluorescence and spectroscopy. J Phys Chem C. 2011;115(22):10955–63. doi: 10.1021/jp111820b.
[30] Xie J, Zheng Y, Ying JY. Highly selective and ultrasensitive detection of Hg(2+) based on fluorescence quenching of Au nanoclusters by Hg(2+)-Au(+) interactions. Chem Commun (Camb). 2010;46(6):961–3. doi: 10.1039/b920748a. Cai Y, Yan L, Liu G, Yuan H, Xiao D. In-situ synthesis of fluorescent gold nanoclusters with electrospun fibrous membrane and application on Hg (II) sensing. Biosens Bioelectron 2013;41:875–9. 10.1016/j.bios.2012.08.064.
[31] Cao D, Fan J, Qiu J, Tu Y, Yan J. Masking method for improving selectivity of gold nanoclusters in fluorescence determination of mercury and copper ions. Biosens Bioelectron. 2013;42:47–50. doi: 10.1016/j.bios.2012.10.084.
[32] Aswathy B, Sony G. Cu2 + modulated BSA–Au nanoclusters: A versatile fluorescence turn-on sensor for dopamine. Microchem J. 2014;116:151–6. doi: 10.1016/j.microc.2014.04.016.
[33] Wang CW, Chen YN, Wu BY, Lee CK, Chen YC, Huang YH, et al. Sensitive detection of cyanide using bovine serum albumin-stabilized cerium/gold nanoclusters. Anal Bioanal Chem. 2016;408(1):287–94. doi: 10.1007/s00216-015-9104-5.
[34] Lin H, Li L, Lei C, Xu X, Nie Z, Guo M, et al. Immune-independent and label-free fluorescent assay for Cystatin C detection based on protein-stabilized Au nanoclusters. Biosens Bioelectron. 2013;41:256–61. doi: 10.1016/j.bios.2012.08.030.
[35] Feng D-Q, Chen M, Liu G, Zhu W, Sun W, Zhu R, et al. A novel resonance light scattering sensing for glucose based on the conversion of gold nanoclusters into gold nanoparticles. Sens Actuators B Chem. 2015;219:133–8. doi: 10.1016/j.snb.2015.05.019. Wang YW, Tang S, Yang HH, Song H. A novel colorimetric assay for rapid detection of cysteine and Hg(2)(+) based on gold clusters. Talanta. 2016;146:71–4. 10.1016/j.talanta.2015.08.015.
[36] Vericat C, Vela ME, Benitez G, Carro P, Salvarezza RC. Self-assembled monolayers of thiols and dithiols on gold: new challenges for a well-known system. Chem Soc Rev. 2010;39(5):1805–34. doi: 10.1039/b907301a.
[37] Chen Y, Yang T, Pan H, Yuan Y, Chen L, Liu M, et al. Photoemission mechanism of water-soluble silver nanoclusters: ligand-to-metal-metal charge transfer vs strong coupling between surface plasmon and emitters. J Am Chem Soc. 2014;136(5):1686–9. doi: 10.1021/ja407911b.
[38] Kovacs-Nolan J, Phillips M, Mine Y. Advances in the value of eggs and egg components for human health. J Agric Food Chem. 2005;53(22):8421–31. Hacohen N, Ip CJX, Gordon R. Analysis of egg white protein composition with double nanohole optical tweezers. ACS Omega. 2018;3(5):5266–72. 10.1021/acsomega.8b00651.
[39] Joseph D, Geckeler KE. Synthesis of highly fluorescent gold nanoclusters using egg white proteins. Colloids Surf B Biointerfaces. 2014;115:46–50. doi: 10.1016/j.colsurfb.2013.11.017.
[40] Selvaprakash K, Chen YC. Using protein-encapsulated gold nanoclusters as photoluminescent sensing probes for biomolecules. Biosens Bioelectron. 2014;61:88–94. doi: 10.1016/j.bios.2014.04.055.
[41] Li M, Yang D-P, Wang X, Lu J, Cui D. Mixed protein-templated luminescent metal clusters (Au and Pt) for H2O2 sensing. Nanoscale Res Lett. 2013;8(1):1–5.
[42] Selvaprakash K, Chen YC. Detection of ricin by using gold nanoclusters functionalized with chicken egg white proteins as sensing probes. Biosens Bioelectron. 2017;92:410–6. doi: 10.1016/j.bios.2016.10.086.
[43] Zhang F, Liu M, Liu R, Li J, Sang Y, Tang Y, et al. A broad-spectrum sensing strategy for the tetracycline family of antibiotics based on an ovalbumin-stabilized gold nanocluster and its application in a pump-free microfluidic sensing platform. Biosens Bioelectron. 2021;171:112701. doi: 10.1016/j.bios.2020.112701.
[44] Shao C, Yuan B, Wang H, Zhou Q, Li Y, Guan Y, et al. Eggshell membrane as a multimodal solid state platform for generating fluorescent metal nanoclusters. J Mater Chem. 2011;21(9):8421–31. doi: 10.1039/c0jm04071a.
[45] Tan F, Xie X, Xu A, Deng K, Zeng Y, Yang X, et al. Fabricating and regulating peroxidase-like activity of eggshell membrane-templated gold nanoclusters for colorimetric detection of staphylococcal enterotoxin B. Talanta. 2019;194:634–42. doi: 10.1016/j.talanta.2018.10.031.
[46] Woll AK, Schutz J, Zabel J, Hubbuch J. Analysis of phase behavior and morphology during freeze-thaw applications of lysozyme. Int J Pharm. 2019;555:153–64. doi: 10.1016/j.ijpharm.2018.11.047.
[47] Wei H, Wang Z, Yang L, Tian S, Hou C, Lu Y. Lysozyme-stabilized gold fluorescent cluster: Synthesis and application as Hg(2 +) sensor. Analyst. 2010;135(6):1406–10. doi: 10.1039/c0an00046a.
[48] Lin Y-H, Tseng W-L. Ultrasensitive sensing of Hg2+ and CH3Hg+ based on the fluorescence quenching of lysozyme type VI-stabilized gold nanoclusters. Anal Chem. 2010;82(22):9194–200.
[49] Chen TH, Tseng WL. (Lysozyme type VI)-stabilized Au8 clusters: synthesis mechanism and application for sensing of glutathione in a single drop of blood. Small. 2012;8(12):1912–9. doi: 10.1002/smll.201102741.
[50] Chen W-Y, Lin J-Y, Chen W-J, Luo L, Wei-Guang Diau E, Chen Y-CJN. Functional gold nanoclusters as antimicrobial agents for antibiotic-resistant bacteria. Nanomed. 2010;5(5):755–64.
[51] Lu D, Liu L, Li F, Shuang S, Li Y, Choi MM, et al. Lysozyme-stabilized gold nanoclusters as a novel fluorescence probe for cyanide recognition. Spectrochim Acta A Mol Biomol Spectrosc. 2014;121:77–80. doi: 10.1016/j.saa.2013.10.009.
[52] Olsen JV, Ong SE, Mann M. Trypsin cleaves exclusively C-terminal to arginine and lysine residues. Mol Cell Proteom. 2004;3(6):608–14. doi: 10.1074/mcp.T400003-MCP200.
[53] Kawasaki H, Yoshimura K, Hamaguchi K, Arakawa R. Trypsin-stabilized fluorescent gold nanocluster for sensitive and selective Hg2+ detection. Anal Sci. 2011;27(6):591.
[54] Jin KS, Rho Y, Kim J, Kim H, Kim IJ, Ree M. Synchrotron small-angle X-ray scattering studies of the structure of porcine pepsin under various pH conditions. J Phys Chem B. 2008;112(49):15821–7.
[55] Kawasaki H, Hamaguchi K, Osaka I, Arakawa R. ph-dependent synthesis of pepsin-mediated gold nanoclusters with blue green

and red fluorescent emission. Adv Funct Mater. 2011;21(18):3508–15. doi: 10.1002/adfm.201100886.
[56] Zhuang QQ, Deng HH, He SB, Peng HP, Lin Z, Xia XH, et al. Immunoglobulin G-encapsulated gold nanoclusters as fluorescent tags for dot-blot immunoassays. ACS Appl Mater Interfaces. 2019;11(35):31729–34. doi: 10.1021/acsami.9b11599.
[57] Xue JH, Xiao KP, Wang YS, Liu L, Li JQ, Li M, et al. Aggregation-induced photoluminescence enhancement of protamine-templated gold nanoclusters for 1-hydroxypyrene detection using 9-hydroxyphenanthrene as a sensitizer. Colloids Surf B Biointerfaces. 2020;189:110873. doi: 10.1016/j.colsurfb.2020.110873.
[58] Welinder KG. Covalent structure of the glycoprotein horseradish peroxidase (EC 1.11. 1.7). FEBS Lett. 1976;72(1):19–23.
[59] Bilal M, Barcelo D, Iqbal HMN. Nanostructured materials for harnessing the power of horseradish peroxidase for tailored environmental applications. Sci Total Environ. 2020;749:142360. doi: 10.1016/j.scitotenv.2020.142360.
[60] Wen F, Dong Y, Feng L, Wang S, Zhang S, Zhang X. Horseradish peroxidase functionalized fluorescent gold nanoclusters for hydrogen peroxide sensing. Anal Chem. 2011;83(4):1193–6. doi: 10.1021/ac1031447.
[61] Lee MJ, Song JA, Choi JH, Shin JH, Myeong JW, Lee KP, et al. Horseradish peroxidase-encapsulated fluorescent bio-nanoparticle for ultra-sensitive and easy detection of hydrogen peroxide. Biosensors (Basel). 2023;13(2):15821–7. doi: 10.3390/bios13020289.
[62] Milosevic J, Jankovic B, Prodanovic R, Polovic N. Comparative stability of ficin and papain in acidic conditions and the presence of ethanol. Amino Acids. 2019;51(5):829–38. doi: 10.1007/s00726-019-02724-3.
[63] Chen Y, Wang Y, Wang C, Li W, Zhou H, Jiao H, et al. Papain-directed synthesis of luminescent gold nanoclusters and the sensitive detection of Cu2+. J Colloid Interface Sci. 2013;396:63–8. doi: 10.1016/j.jcis.2013.01.031.
[64] Chen Y, Qiao J, Liu Q, Zhang M, Qi L. Fluorescence turn-on assay for detection of serum D-penicillamine based on papain@AuNCs-Cu(2+) complex. Anal Chim Acta. 2018;1026:133–9. doi: 10.1016/j.aca.2018.04.014.
[65] Jafari M, Tashkhourian J, Absalan G. Electrochemical sensing of D-penicillamine on modified glassy carbon electrode by using a nanocomposite of gold nanoparticles and reduced graphene oxide. J Iran Chem Soc. 2017;14(6):1253–62. doi: 10.1007/s13738-017-1076-2.
[66] Yu T, Xu C, Qiao J, Zhang R, Qi L. Green synthesis of gold nanoclusters using papaya juice for detection of l-lysine. Chin Chem Lett. 2019;30(3):660–3. doi: 10.1016/j.cclet.2018.10.001.
[67] Hong C, Ye S, Dai C, Wu C, Chen L, Huang Z. Sensitive and on-site detection of glyphosate based on papain-stabilized fluorescent gold nanoclusters. Anal Bioanal Chem. 2020;412(29):8177–84. doi: 10.1007/s00216-020-02952-7.
[68] Nishinari K, Fang Y, Guo S, Phillips GO. Soy proteins: A review on composition, aggregation and emulsification. Food Hydrocoll. 2014;39:301–18. doi: 10.1016/j.foodhyd.2014.01.013.
[69] Ling S, Liang H, Li Z, Ma L, Yao J, Shao Z, et al. Soy protein-directed one-pot synthesis of gold nanomaterials and their functional conductive devices. J Mater Chem B. 2016;4(21):3643–50. doi: 10.1039/c6tb00616g.
[70] Zhang L, Wang J, Zhu GN. Pubertal exposure to bismerthlazol inhibits thyroid function in juvenile female rats. Exp Toxicol Pathol. 2009;61(5):453–9. doi: 10.1016/j.etp.2008.10.011.
[71] Wu J, Zhang H, Wang K, Wang C. Determination and study on dissipation and residue of bismerthiazol and its metabolite in Chinese cabbage and soil. Environ Monit Assess. 2014;186(2):1195–202. doi: 10.1007/s10661-013-3449-z.
[72] Li Z, Peng H, Liu J, Tian Y, Yang W, Yao J, et al. Plant protein-directed synthesis of luminescent gold nanocluster hybrids for tumor imaging. ACS Appl Mater Interfaces. 2018;10(1):83–90. doi: 10.1021/acsami.7b13088.
[73] Dan Q, Yuan Z, Zheng S, Ma H, Luo W, Zhang L, et al. Gold nanoclusters-based NIR-II photosensitizers with catalase-like activity for boosted photodynamic therapy. Pharmaceutics. 2022;14(8):15821–7. doi: 10.3390/pharmaceutics14081645.
[74] Xi H, Li N, Shi Z, Wu P, Pan N, Wang D, et al. A three-dimensional "turn-on" sensor array for simultaneous discrimination of multiple heavy metal ions based on bovine serum albumin hybridized fluorescent gold nanoclusters. Anal Chim Acta. 2022;1220:340023. doi: 10.1016/j.aca.2022.340023.
[75] Niu Y, Ding T, Liu J, Zhang G, Tong L, Cheng X, et al. Fluorescence switch of gold nanoclusters stabilized with bovine serum albumin for efficient and sensitive detection of cysteine and copper ion in mice with Alzheimer's disease. Talanta. 2021;223:121745. doi: 10.1016/j.talanta.2020.121745.
[76] Poderys V, Jarockyte G, Bagdonas S, Karabanovas V, Rotomskis R. Protein-stabilized gold nanoclusters for PDT: ROS and singlet oxygen generation. J Photochem Photobiol B. 2020;204:111802. doi: 10.1016/j.jphotobiol.2020.111802.
[77] Peng J, Su Y, Huang FQ, Zuo Q, Yang L, Li J, et al. A simple and rapid fluorescent approach for flavonoids sensor based on gold nanoclusters. J Colloid Interface Sci. 2019;539:175–83. doi: 10.1016/j.jcis.2018.12.042.
[78] Ni P, Liu S, Wang B, Chen C, Jiang Y, Zhang C, et al. Light-responsive Au nanoclusters with oxidase-like activity for fluorescent detection of total antioxidant capacity. J Hazard Mater. 2021;411:125106. doi: 10.1016/j.jhazmat.2021.125106.
[79] Halawa MI, Gao W, Saqib M, Kitte SA, Wu F, Xu G. Sensitive detection of alkaline phosphatase by switching on gold nanoclusters fluorescence quenched by pyridoxal phosphate. Biosens Bioelectron. 2017;95:8–14. doi: 10.1016/j.bios.2017.03.073.
[80] Bothra S, Upadhyay Y, Kumar R, Ashok Kumar SK, Sahoo SK. Chemically modified cellulose strips with pyridoxal conjugated red fluorescent gold nanoclusters for nanomolar detection of mercuric ions. Biosens Bioelectron. 2017;90:329–35. doi: 10.1016/j.bios.2016.11.066.
[81] Hada AM, Craciun AM, Focsan M, Borlan R, Soritau O, Todea M, et al. Folic acid functionalized gold nanoclusters for enabling targeted fluorescence imaging of human ovarian cancer cells. Talanta. 2021;225:121960. doi: 10.1016/j.talanta.2020.121960.
[82] Yan X, Li H, Hu T, Su X. A novel fluorimetric sensing platform for highly sensitive detection of organophosphorus pesticides by using egg white-encapsulated gold nanoclusters. Biosens Bioelectron. 2017;91:232–7. doi: 10.1016/j.bios.2016.11.058.
[83] Akyuz E, Sen FB, Bener M, Baskan KS, Apak R. A novel gold nanocluster-based fluorometric biosensor for measuring prooxidant activity with a large Stokes shift. Talanta. 2020;208:120425. doi: 10.1016/j.talanta.2019.120425.
[84] Zhang Y, Jiang J, Li M, Gao P, Shi L, Zhang G, et al. Bright far-red/near-infrared gold nanoclusters for highly selective and ultrasensitive detection of Hg2+. Sens Actuators B: Chem. 2017;238:683–92. doi: 10.1016/j.snb.2016.07.118.
[85] Tseng WB, Rau JY, Chiou HC, Tseng WL. Synthesis of gold nanoclusters-loaded lysozyme nanoparticles for ratiometric

fluorescent detection of cyanide in tap water, cyanogenic glycoside-containing plants, and soils. Environ Res. 2022;207:112144. doi: 10.1016/j.envres.2021.112144.

[86] Li K, Zhuang P, Tao B, Li D, Xing X, Mei X. Ultra-small lysozyme-protected gold nanoclusters as nanomedicines inducing osteogenic differentiation. Int J Nanomedicine. 2020;15:4705–16. doi: 10.2147/IJN.S241163.

[87] Li W, Xingzhuo Z, Yan W, Wang R, Yang Z, Hu Y, et al. Lysozyme-encapsulated gold nanoclusters for ultrasensitive detection of folic acid and *in vivo* imaging. Talanta. 2023;251:123789. doi: 10.1016/j.talanta.2022.123789.

[88] Bothra S, Babu LT, Paira P, Ashok Kumar SK, Kumar R, Sahoo SK. A biomimetic approach to conjugate vitamin B(6) cofactor with the lysozyme cocooned fluorescent AuNCs and its application in turn-on sensing of zinc(II) in environmental and biological samples. Anal Bioanal Chem. 2018;410(1):201–10. doi: 10.1007/s00216-017-0710-2.

[89] Ghosh S, Bhamore JR, Malek NI, Murthy ZVP, Kailasa SK. Trypsin mediated one-pot reaction for the synthesis of red fluorescent gold nanoclusters: Sensing of multiple analytes (carbidopa, dopamine, Cu(2+), Co(2+) and Hg(2+) ions). Spectrochim Acta A Mol Biomol Spectrosc. 2019;215:209–17. doi: 10.1016/j.saa.2019.02.078.

[90] Fan J, Li R, Xu P, Di J, Tu Y, Yan J. Sensitive sulfide sensor with a trypsin-stabilized gold nanocluster. Anal Sci. 2014;30(4):457–62.

[91] Liu W, Zhang H, Dong X, Sun Y. Composite of gold nanoclusters and basified human serum albumin significantly boosts the inhibition of Alzheimer's beta-amyloid by photo-oxygenation. Acta Biomater. 2022;144:157–67. doi: 10.1016/j.actbio.2022.03.019.

[92] Santhosh M, Chinnadayyala SR, Kakoti A, Goswami P. Selective and sensitive detection of free bilirubin in blood serum using human serum albumin stabilized gold nanoclusters as fluorometric and colorimetric probe. Biosens Bioelectron. 2014;59:370–6. doi: 10.1016/j.bios.2014.04.003.

[93] Zang J, Li C, Zhou K, Dong H, Chen B, Wang F, et al. Nanomolar Hg(2+) detection using beta-lactoglobulin-stabilized fluorescent gold nanoclusters in beverage and biological media. Anal Chem. 2016;88(20):10275–83. doi: 10.1021/acs.analchem.6b03011.

[94] Bhamore JR, Murthy ZVP, Kailasa SK. Fluorescence turn-off detection of spermine in biofluids using pepsin mediated synthesis of gold nanoclusters as a probe. J Mol Liq. 2019;280:18–24. doi: 10.1016/j.molliq.2019.01.132.

[95] He F, Qin X, Bu L, Fu Y, Tan Y, Chen C, et al. Study on the bioelectrochemistry of a horseradish peroxidase-gold nanoclusters bionanocomposite. J Electroanal Chem. 2017;792:39–45. doi: 10.1016/j.jelechem.2017.03.033.

[96] Wang L, Chen G, Zeng G, Liang J, Dong H, Yan M, et al. Fluorescent sensing of sulfide ions based on papain-directed gold nanoclusters. N J Chem. 2015;39(12):9306–12. doi: 10.1039/c5nj01783a.

[97] Kundu A, Park B, Ray C, Oh J, Jun SC. Environmentally benign and cost-effective synthesis of water soluble red light emissive gold nanoclusters: Selective and ultra-sensitive detection of mercuric ions. N J Chem. 2019;43(2):900–6. doi: 10.1039/c8nj02897d.

[98] Liu J, Gan L, Yang X. Glutenin-directed gold nanoclusters employed for assaying vitamin B1. N J Chem. 2020;44(2):487–91. doi: 10.1039/c9nj04570h.

[99] He X, Deng H, Hwang HM. The current application of nanotechnology in food and agriculture. J Food Drug Anal. 2019;27(1):1–21. doi: 10.1016/j.jfda.2018.12.002.

[100] Kaliraj L, Ahn JC, Rupa EJ, Abid S, Lu J, Yang DC. Synthesis of panos extract mediated ZnO nano-flowers as photocatalyst for industrial dye degradation by UV illumination. J Photochem Photobiol B. 2019;199:111588. doi: 10.1016/j.jphotobiol.2019.111588.

[101] Kadam D, Momin B, Palamthodi S, Lele SS. Physicochemical and functional properties of chitosan-based nano-composite films incorporated with biogenic silver nanoparticles. Carbohydr Polym. 2019;211:124–32. doi: 10.1016/j.carbpol.2019.02.005.

[102] Yusefi M, Shameli K, Su Yee O, Teow SY, Hedayatnasab Z, Jahangirian H, et al. Green synthesis of Fe(3)O(4) nanoparticles stabilized by a Garcinia mangostana Fruit peel extract for hyperthermia and anticancer activities. Int J Nanomedicine. 2021;16:2515–32. doi: 10.2147/IJN.S284134.

[103] Xu H, Yang X, Li G, Zhao C, Liao X. Green synthesis of fluorescent carbon dots for selective detection of tartrazine in food samples. J Agric Food Chem. 2015;63(30):6707–14. doi: 10.1021/acs.jafc.5b02319.

[104] Desai ML, Basu H, Saha S, Singhal RK, Kailasa SK. One pot synthesis of fluorescent gold nanoclusters from Curcuma longa extract for independent detection of Cd2+, Zn2+ and Cu2+ ions with high sensitivity. J Mol Liq. 2020;304:112697. doi: 10.1016/j.molliq.2020.112697.

[105] Zhou W, Cao Y, Sui D, Guan W, Lu C, Xie J. Ultrastable BSA-capped gold nanoclusters with a polymer-like shielding layer against reactive oxygen species in living cells. Nanoscale. 2016;8(18):9614–20. doi: 10.1039/c6nr02178f.

[106] Hikosou D, Saita S, Miyata S, Miyaji H, Furuike T, Tamura H, et al. Aggregation/self-assembly-induced approach for efficient AuAg bimetallic nanocluster-based photosensitizers. J Phys Chem C. 2018;122(23):12494–501. doi: 10.1021/acs.jpcc.8b02373; Zhang T-X, Liu H-J, Chen Y. Ultrabright gold-silver bimetallic nanoclusters: Synthesis and their potential application in cysteine sensing. Colloids Surf A Physicochem Eng Asp. 2018;555:572–9. 10.1016/j.colsurfa.2018.07.038.

[107] Zhang N, Si Y, Sun Z, Chen L, Li R, Qiao Y, et al. Rapid, selective, and ultrasensitive fluorimetric analysis of mercury and copper levels in blood using bimetallic gold-silver nanoclusters with "silver effect"-enhanced red fluorescence. Anal Chem. 2014;86(23):11714–21. doi: 10.1021/ac503102g.

[108] Mora-Sanz V, Saa L, Briz N, Moller M, Pavlov V. Antibody-directed synthesis of catalytic nanoclusters for bioanalytical assays. ACS Appl Mater Interfaces. 2020;12(26):28993–9. doi: 10.1021/acsami.0c05229; Liu H, Zhu N, Li M, Huang X, Wu P, Hu Z, et al. Induced fluorescent enhancement of protein-directed synthesized gold nanoclusters for selective and sensitive detection of flame retardants. Sci Total Environ. 2020;713:136488. doi: 10.1016/j.scitotenv.2019.136488.